



Lawrence Berkeley Laboratory

UNIVERSITY OF CALIFORNIA

Materials & Molecular Research Division

RECEIVED
LAWRENCE
BERKELEY LABORATORY

APR 15 1983

LIBRARY AND
DOCUMENTS SECTION

Submitted to the Journal of Chemical Physics

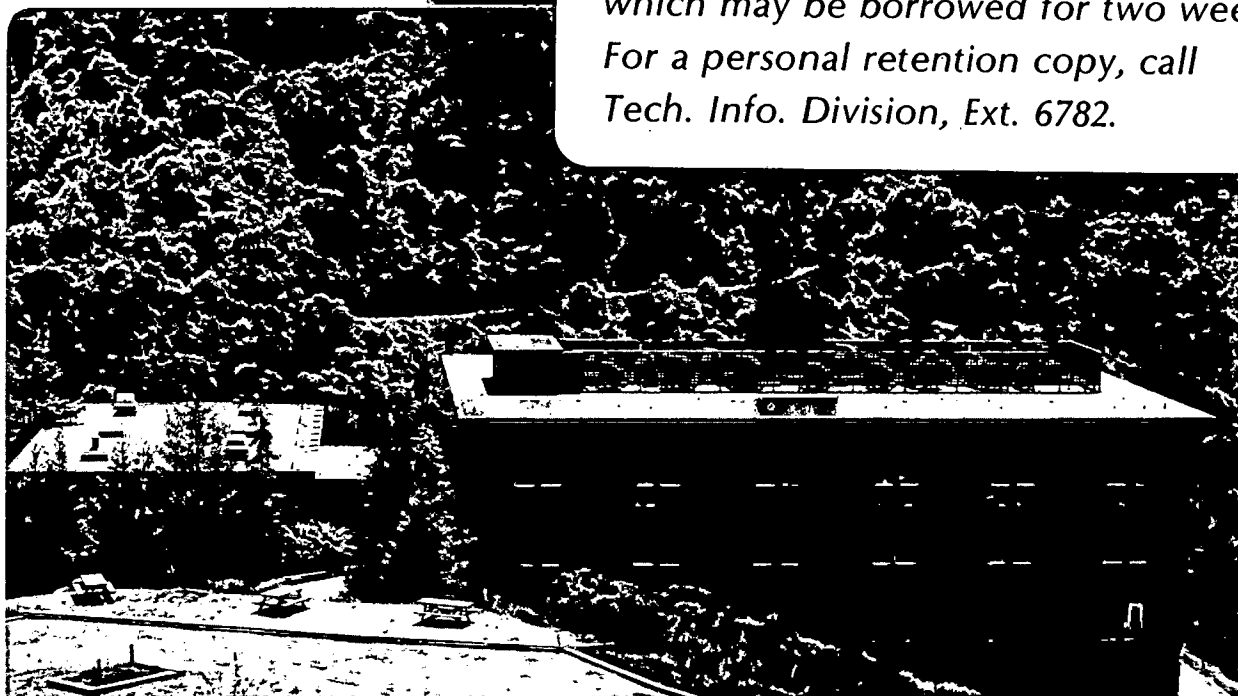
ENERGY REDISTRIBUTION AMONG INTERNAL STATES OF
NITRIC OXIDE MOLECULES UPON SCATTERING FROM
Pt(111) CRYSTAL SURFACE

M. Asscher, W.L. Guthrie, T.-H. Lin,
and G.A. Somorjai

January 1983

TWO-WEEK LOAN COPY

*This is a Library Circulating Copy
which may be borrowed for two weeks.
For a personal retention copy, call
Tech. Info. Division, Ext. 6782.*



LBL-15779
e-2

DISCLAIMER

This document was prepared as an account of work sponsored by the United States Government. While this document is believed to contain correct information, neither the United States Government nor any agency thereof, nor the Regents of the University of California, nor any of their employees, makes any warranty, express or implied, or assumes any legal responsibility for the accuracy, completeness, or usefulness of any information, apparatus, product, or process disclosed, or represents that its use would not infringe privately owned rights. Reference herein to any specific commercial product, process, or service by its trade name, trademark, manufacturer, or otherwise, does not necessarily constitute or imply its endorsement, recommendation, or favoring by the United States Government or any agency thereof, or the Regents of the University of California. The views and opinions of authors expressed herein do not necessarily state or reflect those of the United States Government or any agency thereof or the Regents of the University of California.

ENERGY REDISTRIBUTION AMONG INTERNAL STATES OF NITRIC OXIDE MOLECULES UPON
SCATTERING FROM Pt(111) CRYSTAL SURFACE

M. Asscher, W.L. Guthrie, T.-H. Lin and G.A. Somorjai

Materials and Molecular Research Division
Lawrence Berkeley Laboratory

and

Department of Chemistry
University of California, Berkeley
Berkeley, California 94720

This manuscript was printed from originals provided by the authors.

ABSTRACT

The internal states distributions, rotation and vibration, of nitric oxide molecules scattered from the Pt(111) crystal surface are reported. These distributions were measured as a function of crystal temperature (T_g) and scattering angles. The extent of equilibration of the three degrees of freedom, e.g. translation, rotation and vibration with the metal surface is discussed in terms of the energy accommodation coefficients, γ . It was found that $\gamma_{trans} > \gamma_{vib} > \gamma_{rot}$. A model is suggested to account for the cold rotational distribution of molecules scattered via a trapping desorption mechanism. The vibrational distributions are determined by kinetic effects and by the competition between vibrational excitation of the adsorbed molecules and their desorption.

INTRODUCTION

One of the main goals of modern surface science research is to unravel the molecular details of energy transfer between gas phase molecules and the solid surface. This way, the elementary surface processes, adsorption, molecular rearrangement on the surface and desorption that are always dominant parts of any surface reaction can be studied separately and perhaps controlled to achieve optimum rates and selectivity of reaction path. In recent years, new instrumentation permitted the determination of the velocity distribution of the incident and scattered molecules by time of flight measurements using molecular beam-surface scattering.⁽¹⁾ including the NO/Pt(111) system ⁽²⁾. Thus, the energy transfer between the vibrating surface atoms and the scattering molecules could be determined as a function of surface temperature, surface structure and incident and scattering angles. Shortly thereafter, laser induced fluorescence was applied to the measurement of the rotational energy distribution of molecules scattered from solid surfaces.⁽³⁻⁷⁾

In this paper we report the application of two photon ionization to determine the rotational and vibrational energy distribution of incident and scattered NO molecules from the (111) crystal face of platinum during the molecular beam-surface scattering experiments. Using internally cold incident NO molecules from a nozzle beam, the internal excitation of the scattered molecules was measured as a function of surface temperature and scattered angle. Two photon ionization proved to be a very sensitive state selective detection technique that permits simultaneous monitoring of the rotational and vibrational energy states of the NO molecules. As a result of these studies, for the first time, we obtained for the NO/Pt(111) system the redistribution of translational, rotational and vibrational energies during surface scattering, which should help the theoretical scrutiny of the elementary surface processes.

We find that the rotational energy accommodation upon surface scattering of NO is relatively poor especially as the surface temperature is increased above 300K. The vibrational energy transfer is somewhat more efficient although still declines with increasing crystal temperature. The translational energy of NO was found previously⁽²⁾ to equilibrate well during surface scattering although it also shows a deviation from the expected Boltzmann distribution with increasing surface temperature.

Molecular models are suggested to rationalize the observed rotational and vibrational energy distribution of NO scattered from the Pt(111) surface.

EXPERIMENTAL

The experiment described here involves the scattering of a supersonic nitric oxide molecular beam from a Pt(111) single crystal surface under ultra-high vacuum (UHV) conditions. The scattered molecules' internal energy is monitored by means of two photon ionization (TPI) excited by a tunable UV laser. The ions are detected with an ion multiplier.

The molecular beam-surface scattering apparatus was described in detail elsewhere.⁽⁸⁾ Pertinent details will be briefly described, with emphasis given to the modifications of the chamber (Fig. 1) made in order to conduct the current experiment. The supersonic molecular beam is generated in a two stage differentially pumped beam source. A nozzle of 0.075 mm diameter is pressurized to 200 torr of NO or a mixture of He and NO at a ratio of four to one. The beam has a cross-sectional diameter of 1.5 mm at the crystal and a flux estimated to be in the $10^{15} \text{cm}^{-2} \text{s}^{-1}$ range for an equivalent pressure of approximately 10^{-5} torr. The characteristic rotational temperature of the molecules in the incident beam was 45K, the translational temperature was 615K (NO) or 1390K (He/NO 4:1 mixture). The incident beam vibrational temperature

was not measured, but it is assumed to be low enough to make only the vibrational ground state population significant. Reactive scattering studies can be conducted through the use of the two separate beam sources. We have measured the internal state distribution of NO produced in the catalytic oxidation of NH_3 , which will be reported elsewhere.⁽⁹⁾

A variable, low frequency chopper was mounted to the primary beam source. The chopper was typically operated at 10 Hz, the optimum repetition rate of the laser, and the laser was triggered and synchronized by an optical trigger attached to the chopper. At a chopper frequency of 10 Hz, the molecular beam pulse duration was 5 msec with a rise time of ca. 0.25 msec. The beam chopper limited the incident NO flux to those times immediately around the time of sampling of the scattered flux by the laser pulse. This lowered the background NO pressure in the main chamber, and lowered the rate of contamination of the crystal by the beam.

The base pressure of the UHV scattering chamber was 2.5×10^{-10} torr, but rose to 5×10^{-10} torr with the beam present.

The Pt(111) sample is a disc of 0.7 cm diameter and 0.3 mm thickness. The crystal was heated by electron bombardment, and temperatures were monitored by a Pt/Pt 10% Rh thermocouple spot-welded to the crystal. Auger electron spectroscopy (AES) with a retarding field analyzer was used to determine the crystal cleanliness. The crystal was cleaned between experiments or during an experiment, when necessary for longer or high temperature experiments, by an Ar^+ ion sputtering gun. C, O and Ca atoms were the only surface contaminants observable by AES. At the end of the experiments the observed contaminant coverages were less than 0.02, 0.1, and 0.05 monolayers for C, O, and Ca respectively.

The ion detector consists of a 20 stage ion multiplier (Hamamatsu, R-595)

typically operated at 2500 - 3500 V bias, and a 12.5 cm focal length lens. The lens is moveable and this motion is used to adjust the position of the focal point along the laser beam path.

As originally designed, the detector assembly was enclosed in a stainless steel tube, differentially pumped by a 60 l/sec ion pump to reduce the background NO pressure in the ionization zone. It was found that stray laser light on neighboring metal and quartz surfaces of the differential chamber produced large background ion currents that masked the NO TPI signal. It was also observed that this surface ion production process was partially thermal in nature, and could be suppressed by cooling of the surfaces involved with liquid nitrogen. Cooling would also help to reduce background NO pressures. However, these modifications were not made for the current experiments, so the study reported here was conducted without differential pumping of the detector.

The detector was mounted in the main chamber on an 18" diameter rotatable flange. The spring-loaded teflon-seal flange is a modified configuration of a design described previously by Wharton and coworkers.⁽¹⁰⁾ The laser beam was aligned externally to the center of the rotatable flange, then deflected 2.5 cm off axis by a pair of prisms, so that rotation of the flange caused rotation of the laser beam with the detector. Rotation of the laser beam focal area in the 2.5 cm radius arc about the crystal provided angular resolution of ca. 1°.

The tunable UV laser system is a Quanta-Ray Nd:YAG (DCR A-1) pumped dye laser (TDL-1) together with a wavelength extension unit (WEX-1). This laser generates the UV radiation by doubling the dye laser frequency through a KD*P crystal and then mixing the doubled frequency with the residual fundamental frequency of the Nd:YAG laser via an additional KD*P crystal. This produces

the tunable radiation near 225 and 236 nm required to excite the $A^2\Sigma^+(v'=0)$ $\leftarrow X^2\Pi_{1/2}(v''=0)$ and $A^2\Sigma^+(v'=0)$ $\leftarrow X^2\Pi_{1/2}(v''=1)$ NO vibronic transitions, respectively. Laser energies at the above wavelengths were 0.7 - 1 mJ/pulse with spectral resolution of about 2 cm^{-1} (FWHM). During a scan of rotational distribution the laser energies were attenuated to be constant at 200 $\mu\text{J/pulse}$. Dispersion in the WEX separating prism caused a deflection of 0.14° in the UV beam direction for every 1 nm of wavelength tuning. This may cause severe experimental problems, therefore a mechanical system was developed to rotate the Pelin-Brocca prism in the WEX to compensate for the deflection.

The laser energy was monitored by two separate photodiodes (EG&G, SGD100). A fraction of the UV intensity was reflected from a quartz window into cells containing sodium-salicylate solution, and the fluorescence from the solution was monitored by the visible light sensitive photodiodes. The output of the first fluorescence cell was measured by a picoammeter for manual monitoring of laser intensity. The current from the second photodiode was digitized in a gated charge-to-digital converter (LeCroy, model 2248) and transferred to a NOVA 2 computer.

The current output from the ion-multiplier consisted of a pulse caused by scattered UV laser light incident on the multiplier, followed after 1 μsec by a pulse of current from the ions arrival at the multiplier. The ion current was extracted by a second gated charge-to-digital converter. The signal processing was performed by the minicomputer, which normalized each ion current pulse by the corresponding laser intensity, and averaged 20 to 200 normalized signal pulses, outputting the average normalized intensity to an X-Y recorder. The computer also controlled the advance of the dye laser grating for the tuning of the UV laser.

RESULTS

Rotational Excitation

Typical vibronic two photon ionization spectra are shown in Fig. 2. Fig. 2a is the spectrum of the incident beam, Fig. 2b is a spectrum of room temperature gas phase NO at a pressure of 5×10^{-8} torr, and Fig. 2c is a typical spectrum of NO molecules scattered from the Pt(111) crystal at $T_s = 580\text{K}$. All three spectra are at a laser wavelength of ~ 226 nm, which corresponds to a one photon absorption of the $A^2\Sigma^+(\nu' = 0) \leftarrow X^2\Pi_{1/2}(\nu'' = 0)$ electronic transition. The assignment of the rotational lines is based on constants and equations suggested in the literature.⁽¹¹⁾ We use the lines in the $R_{11} + Q_{21}$ branch for rotational distribution analysis because this branch has the largest number of non overlapping lines, within our modest resolution, Fig. 2. The incident beam spectrum (Fig. 2a) is achieved by removing the crystal from the beam path and positioning the rotatable flange such that the laser beam intercepts the incident molecular beam.

In analyzing the ground state rotational distribution, it is convenient to assume some rotational population distribution function and to fit the assumed function to the experimental data by varying the functional parameters, thus extracting parameters that will reflect the ground state rotational population. If there is equilibrium between the rotational states, a Boltzmann distribution function should describe the ground state population. If such equilibrium does exist, a plot of the logarithms of the rotational line intensities N_j normalized to the rotational degeneracy $(2j'' + 1)$ and rotational line strength factor S_j versus the rotational energy should result in a straight line:

$$N_{j''} = (2j'' + 1)S_{j''} \exp(-E_{\text{rot}}/kT). \quad (1)$$

In our experimental conditions, which are a typical laser energy of 200 $\mu\text{J}/\text{pulse}$, spectral linewidth of 2 cm^{-1} , and focusing lens of 12.5 cm f.l., the first electronic transition (A + X) of the NO molecule is in saturation, which means that $S_{j''} = 1$ for all j'' and one should normalize by the degeneracy factor only. The saturation conditions, which were observed previously elsewhere,⁽¹²⁾ could easily be seen in our calibration spectra of room temperature NO gas in the chamber (Fig. 2b). Using equation 1 with $S_{j''}=1$ gave rotational temperatures of $290 \text{ K} \pm 20\text{K}$, however using Honl-London⁽¹¹⁾ factors in equation 1 gave rotational temperatures lower than room temperature, $230 \pm 20\text{K}$. It was also observed that by increasing the laser energy, the spectral resolution is gradually decreased from 1.5 cm^{-1} (FWHM) at laser energies of 25 $\mu\text{J}/\text{pulse}$ to $\sim 2 \text{ cm}^{-1}$ at laser energies of 150 $\mu\text{J}/\text{pulse}$ and above. We attribute this effect to saturation broadening. In Fig. 2a and 2b the laser energy is 40 $\mu\text{J}/\text{pulse}$, whereas in Fig. 2c the laser energy is 200 $\mu\text{J}/\text{pulse}$ and the somewhat lower resolution is clear.

In Fig. 3 a typical rotational temperature analysis is shown for NO molecules scattered from the Pt(111) crystal surface at 580K. The incident beam is pure NO having an average translational energy of 0.1 eV. The rotational temperature was measured at two different scattering angles, normal to the surface (filled circles in Fig. 3), and at the specular angle, which is 62° from the normal to the surface (open circles in Fig. 3). Different rotational temperatures T_{rot} were observed at the two scattering angles: $T_{\text{rot}} = 400 \pm 40\text{K}$ for normal, and $T_{\text{rot}} = 480 \pm 40\text{K}$ for the specular scattering angle. Rotational analysis was done also for a slightly higher incident energy beam a He/NO 4:1 seeded beam having an average kinetic energy of $\sim 0.24 \text{ eV}$. The scattered molecules from the crystal at 580K were ionized at the specular angle and a T_{rot}

of $480 \pm 40\text{K}$ was found. This means that an increase in the incident energy by more than twice had no observable effect on the scattered molecules' rotational distribution.

In Fig. 4 a summary of the rotational temperatures is presented. The data points in Fig. 4 are from an incident beam of pure NO with an average translational energy of 0.1 eV. The crosses were measured at the normal angle to the crystal surface, whereas at $T_s = 580\text{K}$ the two measurements at specular angle, that were described above, appear as a single open circle. It is interesting to note that at two of the highest crystal temperatures in which rotational distributions of scattered molecules were measured, $T_s = 820$ and 890K , a significant deviation from a single rotational temperature was observed for $j'' > 20 \frac{1}{2}$. (This information is not included in Fig. 4, but is contained in Table 1 of (14).) An important feature of Fig. 4 is that at all crystal temperatures studied here,⁽¹⁵⁾ the scattered molecules could be characterized for $j'' < 18 \frac{1}{2}$ by rotational temperatures smaller than 450K . Similar observations on the same system were reported recently.⁽¹⁶⁾

In Fig. 5 the angular distribution of scattered NO molecules at different final rotational states is shown. Here the temperature of the Pt(111) crystal surface is 580K . The open circles are of scattered NO molecules at $j'' = 1 \frac{1}{2} - 6 \frac{1}{2}$, namely the band head of the $O_{11} + P_{21}$ transition at 226.26 nm , whereas the filled circles are of scattered NO molecules at $j'' = 15 \frac{1}{2}$ as observed by the $R_{11}(15 \frac{1}{2})$ line at 226.08 nm . Both spectra are dominated by a cosine angular distribution, with a slight increase in the flux evident near the specular angle ($\theta_f = 62^\circ$). This type of angular distribution was reported previously for the NO/Pt(111) system.⁽²⁾ For the higher j'' spectrum, the specular feature is slightly more pronounced, which is consistent with the two different rotational temperatures observed at the normal and specular scattering

angles (Fig. 3).

Vibrational Excitation

By tuning the laser to 236 nm, the $A^2 + (v' = 0) \leftarrow X^2_{1/2} (v'' = 1)$ transition could be excited and therefore the population of the first excited vibrational state could be monitored. The $v''=1$ population could be determined also using the $A(v' = 1) \leftarrow X(v'' = 1)$ transition, but since it overlaps with the high j'' states of the $A(v' = 0) \leftarrow X(v'' = 0)$ transition, high laser resolution is required to distinguish between the two transitions, and the assignment of rotational lines becomes more complex.

In Fig. 6 an angular distribution of vibrationally excited molecules scattered from the Pt(111) surface is presented. The angular distribution of $NO(v'' = 1, j'' = 1/2 - 6 1/2)$ molecules (Fig. 6) is almost a perfect cosine with no sign of the enhancement near the specular angle that was found for ground state molecules (see Fig. 5 and (2)) at $T_g = 820K$.

The relative populations of ground state and vibrationally excited molecules was measured to determine the degree of vibrational excitation of the scattered NO. Ideally, each rotational line of the ground and excited vibrational manifolds should be measured and the intensities summed, but this approach is impractical given the low populations in the $v'' = 1$ level. Instead we have used the intensity of the band head of the $O_{11} + P_{21}$ branch, $j'' = 1/2 - 6 1/2$, as a measure of the vibrational populations. This is justified since the band heads are usually not very sensitive to changes in rotational temperature.⁽¹⁷⁾ Also it was shown for ground state molecules in exact rotational temperature measurements (Fig. 4) and was assumed for $v'' = 1$ molecules by the comparison of the intensity of the P_{11} band head ($j'' = 5 1/2 - 12 1/2$) signal to the $O_{11} + P_{21}$ band head ($j'' = 1/2 - 6 1/2$) signal, that there is only a small

change in the rotational temperature of the scattered molecules as a function of T_g .

The approximate two orders of magnitude difference in populations of the vibrational levels would present problems in the calibration of the ion detector sensitivity, so we made the vibrational measurements as follows. Tuning the laser around 236.28 nm, we could scan over the $Q_{11} + P_{21}$ band head of the scattered NO ($v'' = 1, j'' = 1/2 - 6 1/2$) molecules from the Pt(111) crystal surface at a given temperature (T_g), averaging typically 100 laser pulses for each wavelength. Then we removed the crystal and filled the scattering chamber with room temperature gas phase NO to the pressure that gave the same signal intensity in the hot band transition $A(v' = 0) \leftarrow X(v'' = 1)$ as that of the scattered molecules. This reference signal originates from an effective pressure of NO ($v'' = 1$) molecules that is the measured pressure times the vibrational Boltzmann factor at room temperature, which is 1.05×10^{-4} for $T_v = 295K$ and $E_v = 1876.1 \text{ cm}^{-1}$. The same procedure is then repeated for the scattered ground state molecules by scanning the laser around 226.25 nm, in this case correction for the Boltzmann factor is unnecessary. The ratio between the two effective pressures (or densities) is the population ratio of NO($v'' = 1$) and NO($v'' = 0$) molecules.

A few remarks should be added to make the principle behind these measurements clearer: a) since the two photon ionization process is sensitive to the density of molecules one usually assumes that the velocity distribution is independent of the vibrational state of the molecules so that the relative fluxes are given directly by the densities. This assumption was made implicitly(3,4,6,7) and explicitly(5) in previous works in which rotational excitation of scattered molecules was measured. Otherwise a complete description of the velocity distribution at each vibrational state as a function of T_g is necessary in order to correct from density to flux populations of the scattered

molecules. The velocity distribution of the total flux of scattered NO from the Pt(111) surface was measured previously in this lab.(2)

b.) The vibrational intensities are measured relative to pressure measurements, so the pressure measurements must be linear over several orders of magnitude in the 10^{-6} - 10^{-10} torr range. Using a nude ion gauge or mass spectrometer with reasonable care, this is usually not a difficulty.

c.) The effect of the Frank-Condon factors on the population measurements are eliminated since the same factor affects the intensity of the scattered molecules' signal and the reference signal from the added NO gas. More importantly, two different laser wavelengths are used to ionize the two vibrational states, which may result in different ionization cross sections from the $A^2\Sigma^+(v' = 0)$ state; these unknown factors are also eliminated by this method.

The population ratio measurements were done at four crystal temperatures, $T_g = 620, 820, 990$ and $1155K$. In Fig. 7 the experimental $NO(v'' = 1)/NO(v'' = 0)$ population ratios as a function of T_g are indicated by crosses. Some of the experimental points in Fig. 7 were measured as a relative signal both for the ground (the open circles in Fig. 7) and the vibrationally excited molecules, and the ratios between these signals were then normalized to the directly measured ratios at the four crystal temperatures mentioned above. The open circles at the top of Fig. 7 are the relative signal intensity of the $NO(v'' = 0)$ molecules as a function of T_g , as observed at the normal to the crystal surface. The solid line is the Boltzmann factor $\exp(-E_v/kT_g)$ where $E_v = 1876.1 \text{ cm}^{-1}$. The dashed line that connects the crosses is a fit to the expression $A\exp(-E_v/kT_g)$ with $A = 0.67$ and $E_v = 1876.1 \text{ cm}^{-1}$. Two points should be emphasized in Fig. 7:

a) The fitted expression (dashed line) describes very well our experimental results over a wide crystal temperature range, $450 - 1000K$, which means that the vibrational population ratio is less than the corresponding Boltzmann

factor and that the deviation is a constant, e.g. invariant with crystal temperature. b.) There is a deviation from the fitted expression at $T_s > 1000$ K and the deviation seems to increase with T_s .

In order to compare the extent of vibrational excitation of the strongly interacting NO/Pt(111) system (29 kcal/mole binding energy) to a more weakly interacting system, we exposed the Pt(111) surface to 10 Langmuir of ethylene at $T_s = 450$ K, which decomposes to form a graphitic overlayer. With the graphite on the Pt(111) surface and at $T_s = 820$ K we made an attempt to detect vibrationally excited scattered NO. No observable signal from NO($v'' = 1$) molecules was found. This puts an upper limit of ca. 0.001 to the population ratio of NO($v'' = 1$)/NO($v'' = 0$) for NO molecules scattered from a graphite covered Pt(111) surface at 820K. In a recent study of NO scattered from pure graphite an attempt to observe vibrational excitation was unsuccessful.⁽¹⁸⁾ At the same crystal temperature for a clean Pt(111) surface the observed ratio is 0.024 (Fig. 7).

A different way to express the vibrational excitation is in terms of a vibrational temperature versus T_s as shown in Fig. 8. We can see that the vibrational temperature of the desorbed molecules is colder than T_s but not by more than 100K for $T_s < 1000$ K. In other words the vibrational degree of freedom accommodates better with the surface than the rotational degree (Fig. 4).

DISCUSSION

The NO/Pt(111) system is the first molecular-surface system in which complete experimental data of the scattered molecules' average energy content (e.g. translational,⁽²⁾ rotational and vibrational⁽¹⁴⁾) is available, together with the incident molecules' energy (excluding incident vibrational energy). This unique situation provides the opportunity to have a close look at the

degree of energy transfer and its efficiency for each molecular degree of freedom. Since the average energy content in each of these modes was determined in terms of the vibrational, rotational or translational temperature, it would be convenient to compare the relative efficiency of energy transfer into these degrees of freedom in terms of the accommodation coefficient γ_i :

$$\gamma_i = \frac{T_{\text{scatt}}^i - T_{\text{incident}}^i}{T_s - T_{\text{incident}}^i} \quad (2)$$

for i equal to translation (T), rotation (R) or vibration (V). In fig. 9 the γ_i coefficient is presented as a function of crystal temperature. It is evident from fig. 9 that a relatively efficient energy transfer process takes place during the interaction time of the NO molecules with the Pt(111) crystal surface. The translational mode is the mode most effectively accommodated to the Pt crystal energy (temperature) with $\gamma_T > 0.8$ for $500\text{K} < T_s < 1200\text{K}$, where for $T_s < 700\text{K}$ the accommodation coefficient is unity. The vibrational mode is also highly accommodated but even at the lowest crystal temperature it is not unity. For $425\text{K} < T_s < 1245\text{K}$ we find $\gamma_V = 0.82 \pm 0.09$, slightly decreasing with the increase of T_s , similar to γ_T but at somewhat lower values. The rotational degree of freedom seems to be the least effectively accommodated mode. γ_R decreases with the increase of T_s down to 0.34 at $T_s = 870\text{K}$. It seems as if the translational and vibrational modes have only minor restrictions for free energy flow with the metal crystal and probably small if any dynamical effects during the desorption process. This is not the case for the rotational degree of freedom. In all three modes there are deviations from complete accommodation as shown in fig. 9. These deviations reflect usually the interesting effects from which the microscopic level of the interaction with the metal surface can be studied most effectively.

It should be emphasized though that the above discussion on the extent of energy transfer, based on the magnitude of the accommodation coefficient, can

give only a vague idea as to the molecular level of interaction with the surface, from which the observed accommodation coefficient originates. In particular if the coefficient is small, an efficient energy flow and high degree of accommodation of the molecules when adsorbed on the surface, followed by dynamical effects along the exit channel (desorption) that modify the distributions to the observed ones, cannot be ruled out unless additional information exists.

Whereas the translational energy of scattered NO molecules from the Pt(111) surface was discussed in a previous publication,⁽²⁾ the origin of the observed rotational and vibrational distributions will be discussed below.

Rotational Excitation

Fig. 4 shows that the rotational temperature of scattered NO molecules from the Pt(111) surface lags substantially from the crystal temperature. At the same time, the rotational population distribution function is Boltzmann like over a large crystal temperature range for $j \leq 18 \frac{1}{2}$. Observations of $T_{rot} < T_s$ were reported for all previous molecular-scattering systems in which the scattered molecules' rotational temperature were measured.⁽³⁻⁷⁾ This general behaviour of colder rotational population of scattered molecules from several surfaces (not necessarily metal surfaces) holds for different types of molecular-surface interactions. It was observed in weakly interacting systems where an inelastic scattering mechanism occurs,^(3,4,5,7) in strongly interacting systems like NO/Ru(001)⁽⁶⁾ where desorption from a purely chemisorbed state occurs, and our results for the NO/Pt(111) system. In the case of NO molecules the rotational temperature is only slightly dependent on crystal temperature. It is found that $T_{rot} \sim 330 \pm 120K$ for $300 < T_s < 870K$, with incident translational energy of ca. 0.1 eV (molecular beam studies) and on four different surfaces (Ru(001), Ag(111), Pt(111), C).

In cases of strongly interacting systems the primary scattering mechanism is trapping-desorption, so that rotational excitation can occur during the time of adsorption. The configuration of NO adsorbed on platinum at high temperatures is unknown. It may be in an upright configuration with a chemical bond between the nitrogen atom and the Pt atoms as was reported⁽¹⁹⁾ for $T_s < 350K$, it may adsorb in a nearly free tumbling state, or pass through such a state as its energy increases prior to desorption. In unimolecular reactions theory this situation is referred to as a "loose transition state complex".⁽²⁰⁾ Even if the configuration of the NO may not allow a free rotation, as for instance in the upright bound configuration, an instantaneous rotational motion and energy can still be defined. By simple classical mechanical considerations the motion and kinetic energy of the adsorbed molecule can be separated into a translation of the center of mass and a rotational motion about the center of mass, which can be considered as an instantaneous rotation. The total kinetic energy of the molecule is a sum of the kinetic energies of these two motions. Therefore, the energy in the center of mass motion and in the instantaneous rotational motion about the center of mass should be characterized by a temperature that is equal to the crystal temperature, assuming that the NO molecules have had time to reach equilibrium with the platinum. If NO could be suddenly freed from the surface, the motion prior to separation would lead to some rotational energy, and the distribution of rotational energies should be the equilibrium distribution at the surface temperature. This conclusion is based on the approximation that the rotational motion about the center of mass can be treated classically.

Based on NO desorption rate constants⁽²¹⁾ NO surface residence times should be long enough to reach equilibrium ($>10^{-8}$ sec. for $T_s < 1000K$) so that the cold rotational distributions are possibly due to dynamical effects along

the exit channel (desorption) that generate the observed distribution. We propose two mechanisms that could account for cold rotational distributions. One is based on the assumption that NO can freely rotate on the surface prior to desorption and the second mechanism is based on a restricted rotation or wagging vibration configuration.

One approach is to address the observation of cold rotational distributions in terms of the microscopic reversibility principle. The preferential desorption of rotationally cold molecules implies that the sticking probability of NO molecules is rotational energy dependent, namely molecules with lower rotational energy have higher sticking probabilities, as proposed recently in calculations for NO scattered from Ag(111).⁽²²⁾ Consideration of the adsorption process may provide insight into the mechanism of the desorption. It was found that translational to rotational energy transfer is efficient in inelastic scattering of NO from Ag(111).⁽⁵⁾ Assuming that this effect is the same for the NO/Pt(111) system, then from microscopic reversibility the rotational to translational energy exchange is also efficient, which might in turn lower the sticking probabilities of rotationally energetic molecules. We suggest that this same surface mediated rotational to translational energy transfer may affect the NO desorption. We assume for this mechanism that the NO is free to tumble and that the initially rotationally energetic molecules have an enhanced probability for desorption via the rotational to translational coupling while losing some of their rotational excitation. If the enhancement of the desorption probability for rotationally excited molecules is large enough this mechanism may also deplete the high energy portion of the rotational energy distribution, leading to a non-equilibrium distribution of rotational energies on the surface in a manner analogous to the non-equilibrium desorption mechanism proposed to explain cold translational energies of some desorbates.⁽²³⁾

The second model is based on the perturbed rotational motion or better stated, the wagging vibration of the NO molecule which is now assumed to be bound in an upright configuration with a chemical bond between the nitrogen atom and the surface Pt atoms. The molecule should not necessarily be bound to a fixed site but rather might move on the surface from site to site while in a upright configuration. The distribution of vibrational energy in the nitrogen-metal bond of the O=N-Pt complex is of the Boltzmann type even after a much shorter time as compared with the mean residence time of the NO molecules on the surface at our experimental conditions ($T_s < 870K$). The more energetic molecules that present the high energy tail of the distribution functions are close to the top of the potential well that describes the nitrogen-metal surface bond in the Z direction (perpendicular to the surface). These molecules have the highest probability to absorb a small quantity of energy from the system, which would eventually lead to desorption. The mechanism of energy transfer in this final stage before desorption determines the final, observed rotational excitation and distribution function. This process is sometimes referred to as the "dynamical effects along the exit channel". The NO is a heteronuclear diatomic molecule and is bound through its nitrogen atom to the platinum surface, presumably because of charge distribution that is similar to the CO-metal bond. The wagging vibration (that was previously discussed in terms of instantaneous rotation) is consequently restricted to small changes in the wagging angles even at high crystal temperatures, because at the turning points of the vibration the oxygen atom experiences a repulsion by the metal surface. The following energy transfer mechanism is proposed that could account for a final cold rotational distribution: assuming that the repulsion between the metal surface and the oxygen end of the NO molecule is long range, then even at NO-surface distances that are long enough to consid-

er the molecules already decoupled from the surface or being desorbed, free rotation cannot take place. It is suggested that the repulsion causing the restricted wagging vibration, provides a coupling mechanism between this motion and the O=N-surface stretch. If this coupling is strong then the transition state complex of the desorbing NO molecules is not a "loose complex", where internal modes of the fragments (here the NO and the surface) are considered uncoupled.⁽²⁰⁾ The wagging vibration energy decreases during the desorption process by dumping part of it into the "reaction coordinate", namely the NO-surface bond breaking. Referring to our previous definition of the wagging vibration as an instantaneous rotational motion in equilibrium with the surface, by loosening part of its energy the final rotational distribution is expected to be colder than the crystal temperature. The energy required for the O=N-surface bond breaking need not be provided by the wagging vibration alone, but could also be transferred from the metal surface as well. A more complete energy transfer picture would consider the combination of these two energy sources to contribute different amounts of energy to the molecules in the ensemble of adsorbed species. The overall effect would be a "rotational cooling".

It is interesting to note consequences of this mechanism, or any repulsive interaction on the final rotational distribution of the desorbing molecule. For example, increasing the coverage of NO molecules may also alter the rotational distribution since the interaction between the neighboring molecules is repulsive.

The gas phase kinetics experiments that may be correlated with our studies are IR laser induced multiphoton dissociation of molecules, followed by the rotational (and vibrational) distribution analysis of fragments (24). In some of these studies an average excess energy in the parent molecules prior

to dissociation could be estimated, though there is currently no theoretical basis for predicting a priori how the available energy in the parent molecules will be distributed among products degrees of freedom (24). Correlation between those unimolecular gas phase studies and the desorption dynamics of molecules from surfaces, which may be considered to be a unimolecular process as well might be of great value for better understanding the desorption phenomenon.

The fact that there is a slight angular dependence to the rotational temperature, as shown in Figs. 3 and 5 cannot be understood easily by the cooling mechanisms described above. The enhanced flux of rotationally hot molecules near the specular angle could be related to translational to rotational energy exchange in the fraction of molecules believed to undergo inelastic scattering.⁽²¹⁾ This hypothesis assumes that the inelastically scattered molecules should have more rotational energy than desorbed molecules. In a similar, though somewhat more weakly interacting system of NO from Ag(111),⁽⁵⁾ the inelastically scattered molecules observed at specular angle were found to have a rotational temperature that is colder than the one observed at the normal angle in our system under similar conditions. This implies that an inelastic contribution should lower the rotational temperature, unless we assume that translational to rotational energy transfer is more efficient on Pt than on Ag. We also note that the rotational temperature is unaffected by doubling the incident translational energy. As a supporting evidence for an inelastic rotational excitation, the increased rotational temperature appears to be related to a specular feature in the angular scattering, and this specular feature does not appear in the distribution of the purely trapping-desorption scattering of the NO($v'' = 1$) molecules (see next section and fig. 6).

In order to determine whether the inelastic scattering is responsible for

the enhanced flux of higher j'' states near the specular, an angular distribution should be made at negative scattering angles to see if the enhancement is symmetric. This experiment has not been done. Also, additional rotational distribution spectra should be taken to compare the distributions at specular angle to the distributions at the surface normal at several crystal temperatures.

Vibrational Excitation

The angular distribution of the vibrationally excited NO molecules Fig. 6 is different from the ground state molecules' angular distribution (Fig. 5 and ref. 2 respectively). It is clear that the enhancement of the flux near the specular angle is absent in this spectrum, and the shape is almost purely cosine. As indicated in Figs. 5 and 6, the angular distribution of vibrationally excited molecules was measured at a higher temperature, 820K compared to 580K. From ref. 2 we know that inelastic scattering, and hence the specular feature, is enhanced at higher crystal temperatures, so that the difference between the two angular distributions is more significant. The angular distribution, fig. 6, implies that all the vibrationally excited NO originates from desorbed molecules, and that inelastically scattered molecules cannot be vibrationally excited.

The inelastically scattered molecules stay only one or two vibrational periods of time on the surface before being scattered from it, which is in the 10^{-12} sec time scale. This is apparently too short an interaction time to enable vibrational excitation of the NO molecules by the fluctuating dipoles of the metal surface. The experiment in which a graphitic overlayer was deposited on the Pt(111) surface and an unsuccessful attempt was made to observe vibrationally excited molecules scattered at a crystal temperature of 820K is in a way consistent with the above conclusion. Even though the interaction potential of clean Pt(111) and the graphite covered surface are very different,

it is expected that the molecules could be vibrationally excited on the very weakly interacting graphite covered surface as well, if a long enough residence time was available. With a desorption energy of about 2.8 kcal/mole⁽²⁵⁾ and frequency factor estimated to be ca. 10^{-13} sec⁻¹,⁽¹⁸⁾ a residence time of less than 10^{-12} is expected at $T_g > 700\text{K}$, which is the same order of magnitude as the inelastic interaction times, i.e, too short a time for vibrational excitation. It is important to note that our incident beam energy, 0.1 eV, is too small to excite vibrational states directly ($E_v > 0.23$ eV).

The conclusion that there is minor if any vibrational excitation at surfaces if the interaction times are less than 10^{-12} sec. is not surprising. An interesting question is in what range of residence time does the desorption process start to compete effectively with the vibrational excitation. Experimental evidence that can address this question may provide yet unknown information about the mechanism of a very basic processes in gas phase chemistry, namely the thermal heating of vibrational modes of molecules via collisions with walls, e.g. surfaces.

In Fig. 7 and Fig. 8 one can see a small but increasing deviation of the observed experimental ratio of the excited to ground state populations from the thermal equilibrium ratio at the crystal temperature (e.g. Boltzmann expression) as crystal temperature is increased above 1000 K. This deviation means, we believe, that the rate for vibrational excitation, while still growing with crystal temperature, is increasing slower than the desorption rate and that around 1000 - 1200K the desorption rate constant is comparable in magnitude to the rate constant for vibrational excitation. Using kinetic parameters for the desorption of NO from Pt(111) from⁽²¹⁾ ($E_d = 28.6$ kcal/mole, $\nu = 6 \times 10^{13}$ s⁻¹), residence times of 28 nsec and 2.6 nsec are calculated for crystal temperatures of 1000 and 1200K respectively, assuming first order desorption kinetics, tem-

perature independence preexponential factor (ν), and using the reciprocal of the standard Arrhenius equation

$$k_d^{-1} = \tau = \nu^{-1} \exp(E_d/kT_s) \quad (3)$$

where k_d is the desorption rate constant, τ is the residence time, E_d is the desorption energy and T_s is the crystal temperature. If our interpretation is correct then the desorption starts to compete effectively with the vibrational excitation process at rate constants of about 10^7 - 10^8 sec^{-1} . Assuming that vibrational equilibrium exists on the surface, then the deexcitation rate constant can be determined by the Boltzmann factor which gives values in the range of 10^8 - 10^{10} sec^{-1} .

There are few experiments in which an attempt was made to measure vibrational lifetimes (deexcitation rate constant) of molecules on surfaces from IR line widths, (26) and also theoretical calculations that predict the "damping" rate of vibrationally excited molecules. (27) From the IR measurements on a copper surface a lifetime of 3×10^{-13} sec for the deactivation of an adsorbed methoxy C-H stretch mode is reported. (26) Using dipole interactions the theory (27) predicted lifetimes of ca. 10^{-9} sec. whereas the inclusion of electron-hole excitation mechanism in the metal lead to a lifetime of ca. 10^{-13} sec. The electron-hole excitation mechanism is expected to be important only in free electron type metals like copper and aluminum, therefore it may not be valid for the case of Pt. A different theoretical model, based on electrodynamic calculations successfully predicted vibrational and electronic deexcitation rates of molecules near surfaces (10-1000Å), but separated by dielectric layers (28). We used the formula for the ratio of radiative lifetime rates near the surface to the gas phase value (28) to estimate the deexcitation rate of NO at distance of 2Å from the Pt surface. Using the NO dipole moment (1.5 Debye), the dielectric function for Pt at 0.23eV (the vibrational energy

of NO) (29) and the radiative lifetime of vibrationally excited NO of 80 msec(30), we calculated a deexcitation rate in the range of 10^9 - 10^8 sec⁻¹. This number is close (in order of magnitude estimation) to the deexcitation time inferred from our experiments, with the assumptions that were made before. These results and their interpretation may imply that the above mentioned theory⁽²⁷⁾ is not applicable to all metal surfaces or that an electron-hole deexcitation mechanism could be ruled out in the Pt case. It is interesting to note that as a consequence of our interpretation of the results the vibrational excitation process on the Pt surface seems to be extremely slow as compared to the period of vibrational motion.

The experimental scheme described here may contribute as a complimentary method to the IR technique to study the vibrational excitation and deexcitation of molecules chemisorbed on surfaces. Whereas the IR methods follow the deexcitation process via linewidth measurements, the technique described here is related to the excitation mechanism of molecules on surfaces.

As shown in Fig. 7, the vibrational population ratio of $\text{NO}(v'' = 1)/\text{NO}(v'' = 0)$ as a function of crystal temperature can be described over the surface temperature range of $T_s = 450$ - 950 K by the expression;

$$\text{NO}(v'' = 1)/\text{NO}(v'' = 0) = 0.67\exp(-E_v/kT_s) \quad (4)$$

where $E_v = 1876 \text{ cm}^{-1}$ is the gas phase vibrational energy.⁽¹¹⁾ The constant deviation of the vibrational population ratio from the Boltzmann expression by a factor of 2/3 is beyond the experimental error. It might be rationalized by a model which assumes equilibrium of the N-O stretching vibration on the surface, and first order desorption rates for the molecules in the various vibrational levels. The equilibrium assumption for the vibration is quite reasonable given the long residence times of the NO molecule on the Pt(111) surface - $\tau > 10^{-8}$

sec., and first order desorption kinetics for NO from platinum is generally accepted. If we assume that there may be different desorption rates for the molecules in the two vibrational states, the relative populations of the vibrational levels as observed in the gas phase can be written as

$$\frac{\text{NO}(v'' = 1)}{\text{NO}(v'' = 0)} = \frac{k_d^1}{k_d^0} \times \frac{[\text{NO}(v'' = 1)_{\text{ad}}]}{[\text{NO}(v'' = 0)_{\text{ad}}]} \quad (5)$$

where k_d^1 and k_d^0 are the desorption rate constants for $\text{NO}(v'' = 1)$ and $\text{NO}(v'' = 0)$, while $[\text{NO}(v'' = 1)_{\text{ad}}]$ and $[\text{NO}(v'' = 0)_{\text{ad}}]$ are the concentrations in molecules/cm² of excited and ground state adsorbed NO molecules. Substituting the values for k_d^1 and k_d^0 with the corresponding Arrhenius first order rate constants, and substituting the ratio of vibrational populations with the Boltzmann ratio we have:

$$\frac{\text{NO}(v'' = 1)}{\text{NO}(v'' = 0)} = \frac{v^1 \exp(-E_d^1/kT)}{v^0 \exp(-E_d^0/kT)} \times \exp(-E_{\text{vs}}/kT_s) \quad (6)$$

where v^1 and E_d^1 , and v^0 and E_d^0 are the preexponential factors and desorption energies for the ground and first excited states, and E_{vs} is the surface vibrational energy of the N-O stretch. Combining the exponential terms gives the desired Boltzmann-like expression:

$$\frac{\text{NO}(v'' = 1)}{\text{NO}(v'' = 0)} = \frac{v^1}{v^0} \exp(-E_v'/kT_s) \quad (7)$$

where $E_v' = E_{\text{vs}} + E_d^1 - E_d^0$ is the apparent vibrational energy. This expression reproduces the experimental data if we assume that the ratio v^1/v^0 is independent of temperature. This is an empirical assumption which best matches the constant deviation of the vibrational excitation from a Boltzmann expression. This assumption is justified since preexponential factors are generally expected to have weak temperature dependencies, and it is reasonable to expect that v^0 and v^1 would have roughly the same temperature dependence so that their ratio would be temperature independent.

The meaning of eq. 6 is that across the crystal temperature range of 450-950K there is no competing process to the vibrational excitation, so that there is an exponential increase of the vibrational population ratio.

As shown in Fig. 7 the best fit to the data was given by an apparent vibrational energy E_v' of 1876 cm^{-1} , which is equal to the gas phase energy. Since $E_v' = E_{vs} + E_d^1 - E_d^0$, this implies that E_v' fortuitously equals the gas phase value, or that the two desorption energies are equal and that the vibrational energy in the adsorbed state equals the gas phase vibrational energy. It is quite clear that the vibrational energy of the molecule when adsorbed on the surface must be smaller than the gas phase value, and electron energy loss spectroscopy measurements had shown⁽³¹⁾ that the N-O stretch frequency varies from around 1700 cm^{-1} to around 1800 cm^{-1} depending upon the Pt(111) crystal temperature and the surface coverage. These are far lower temperatures than those used in the current study, therefore we might expect the NO vibrational energy to be nearly equal to the gas phase value, at least at the higher crystal temperature range. It is likely that the same energy for desorption E_d controls the desorption kinetics of the two vibrational states, since the two molecules are almost identical except for the different energy content.

The fit of eq. 6 to the experimental results as shown in Fig. 7 corresponds to preexponential factor ratios of $v^1/v^0 = 0.67$. Fig. 7 and eq. 7 show that an assumption of vibrational equilibrium of the adsorbed NO together with different desorption rate constants for the ground and excited molecules leads to an expression that closely reproduces the data. However this expression implies that the desorption preexponential factors are different, the possible meaning of which is unclear. The common interpretation of these parameters in terms of partition functions or entropy considerations may mean perhaps that the two slightly different molecules (e.g. somewhat longer equilibrium distances for

the excited molecule because of anharmonicity) may have different number of equivalent available sites on the surface, which result in different ν . Further investigations with other crystals and if possible at higher vibrational excited states are necessary to fully understand this point and are in progress at our laboratory.

CONCLUSION

Rotational and vibrational populations of a scattered nitric oxide supersonic molecular beam from a Pt(111) surface were investigated. The rotationally cold scattered molecules were discussed in terms of (a) microscopic reversibility considerations while free to tumble on the surface and (b) a hindered rotation of the adsorbed molecule that is coupled to the N-surface bond. Part of the energy of the wagging vibration (instantaneous rotation) is transferred into this bond during the desorption process, which in turn results in a rotational cooling effect. The vibrational population results were divided into two crystal temperature ranges: at $T_s < 950\text{K}$ the results are interpreted by assuming two different desorption preexponential factors for the two vibrational states, in order to explain the constant deviation from a Boltzmann distribution at the crystal temperature. At $T_s > 1000\text{K}$ an increased deviation from the equilibrated distribution was discussed in terms of a competition between the vibrational excitation and the desorption processes. A vibrational excitation rate constant of ca. $10^7\text{-}10^8 \text{ sec}^{-1}$ was estimated.

ACKNOWLEDGEMENTS

This work was supported by the Director, Office of Energy Research, Office of Basic Energy Sciences, Materials Sciences Division of the U.S. Department of Energy under contract DE-AC03-76SF00098. We acknowledge the San Francisco Laser Center for providing the laser system through NSF grant CHE79-16250. We

would like to thank Professors C.B. Harris and Y.T. Lee for stimulating discussions and Dr. Tim Ling from SFLC and Mr. K. Frank for their advice and technical support. M.A. wishes to thank the Chaim Weizmann Postdoctoral Fellowship Award for providing a postdoctoral fellowship.

REFERENCES

1. M.J. Cardillo, Ann. Rev. Phys. Chem. 32, 331 (1981)
2. W.L. Guthrie, T.-H. Lin, S.T. Ceyer and G.A. Somorjai, J. Chem. Phys. 76 6393 (1982).
3. F. Frankel, J. Hager, W. Krieger, H. Walther, C.T. Campbell, G. Ertl, H. Knipers and K. Segner, Phys. Rev. Lett. 46, 152 (1981).
4. G.M. McClelland, G.D. Kubiak, H.G. Rennagel and R.N. Zare, Phys. Rev. Lett. 46, 831 (1981).
5. A.W. Kleyn, A.C. Luntz and D.J. Auerbach, Phys. Rev. Lett. 47, 1169 (1981); A.C. Luntz, A.W. Kleyn and D.J. Auerbach, J. Chem. Phys. 76, 737 (1982).
6. R.R. Cavanagh and D.S. King, Phys. Rev. Lett. 47, 1829 (1981).
7. J.W. Hepburn, E.J. Northrup, G.L. Ogram, J.C. Polanyi and J.M. Williamson, Chem. Phys. Lett. 85, 127 (1982); D. Etinger, K. Honma, M. Keil and J.C. Polanyi, Chem. Phys. Lett., 87, 413 (1982).
8. S.T. Ceyer, W.J. Siekhaus and G.A. Somorjai, J. Vac. Sci. Technol. 19, 726 (1981).
9. W.L. Guthrie, M. Asscher, T.-H. Lin and G.A. Somorjai, to be published.
10. D.J. Auerbach, C.A. Becker, J.P. Cowin and L. Wharton, Appl. Phys. 14, 141 (1977).
11. R. Engleman, Jr., P.E. Rouse, H.M. Peek and V.D. Balamonte, Los Alamos Scientific Laboratory Report LA-4363 (1970).
12. G.D. Kubiak and R.N. Zare, private communication.
13. W.G. Mallard, J.H. Miller and K.C. Smyth, J. Chem. Phys. 76, 3483 (1982).
14. M. Asscher, W.L. Guthrie, T.-H. Lin and G.A. Somorjai, Phys. Rev. Lett. 49, 76 (1982).
15. At $T_g > 809K$ a rapid contamination growth occurs, mostly of oxygen and calcium atoms.
16. G. Ertl, private communication.
17. M. Asscher, Y. Haas, M.P. Roellig and P.L. Houston, J. Chem. Phys. 72, 768

(1980).

18. F. Frenkel, J. Hager, W. Krieger, H. Walther, B. Ertl, J. Segner and W. Vielhaber, Chem. Phys. Lett. 90, 225 (1982).
19. a) C.M. Comrie, W.H. Weinberg and R.M. Lambert, Surf. Sci. 57, 619 (1976).
b) H. Ibach and S. Lehwald, Surf. Sci. 76, 1 (1978).
20. W. Frost, "Theory of Unimolecular Reactions" in Phys. Chemistry series, Vol. 30 (Academic Press, New York 1973).
21. T.-H. Lin and G.A. Somorjai, Surf. Sci. 107, 573 (1981).
22. J. Tully, to be published.
23. J. Tully, Surf. Sci. 111, 461 (1981).
24. D.S. King in "Dynamics of the Excited State" pg. 105, K.P. Lawley ed., John Wiley & Sons, 1982, and references therein.
25. C.E. Brown and D.G. Hall, J. Colloid Interface Sci. 42, 334 (1973).
26. B.N.J. Persson and R. Ryberg, Phys. Rev. Lett. 48, 549 (1982).
27. B.N.J. Persson, J. Phys. C, 11, 4251 (1978).
28. R.P. Chance, A. Lrock and R. Silbey, Adv. Chem. Phys., 37, 1 (1978);
P.M. Whitmore, H.J. Robota and C.B. Harris, J. Chem. Phys., 76, 740 (1982).
29. A.P. Tenham and D.M. Treherne in "The Optical Properties and Electronic Structure of Metals and Alloys", Proceedings of the International Colloquium, pg. 196, Paris 1965, F. Abeles ed., North Holland, Amsterdam 1966.
30. J.C. Stephenson, J. Chem. Phys., 59, 1523 (1973).
31. J.L. Gland and B.A. Sexton, Surf. Sci. 94, 355 (1980).

FIGURE CAPTIONS

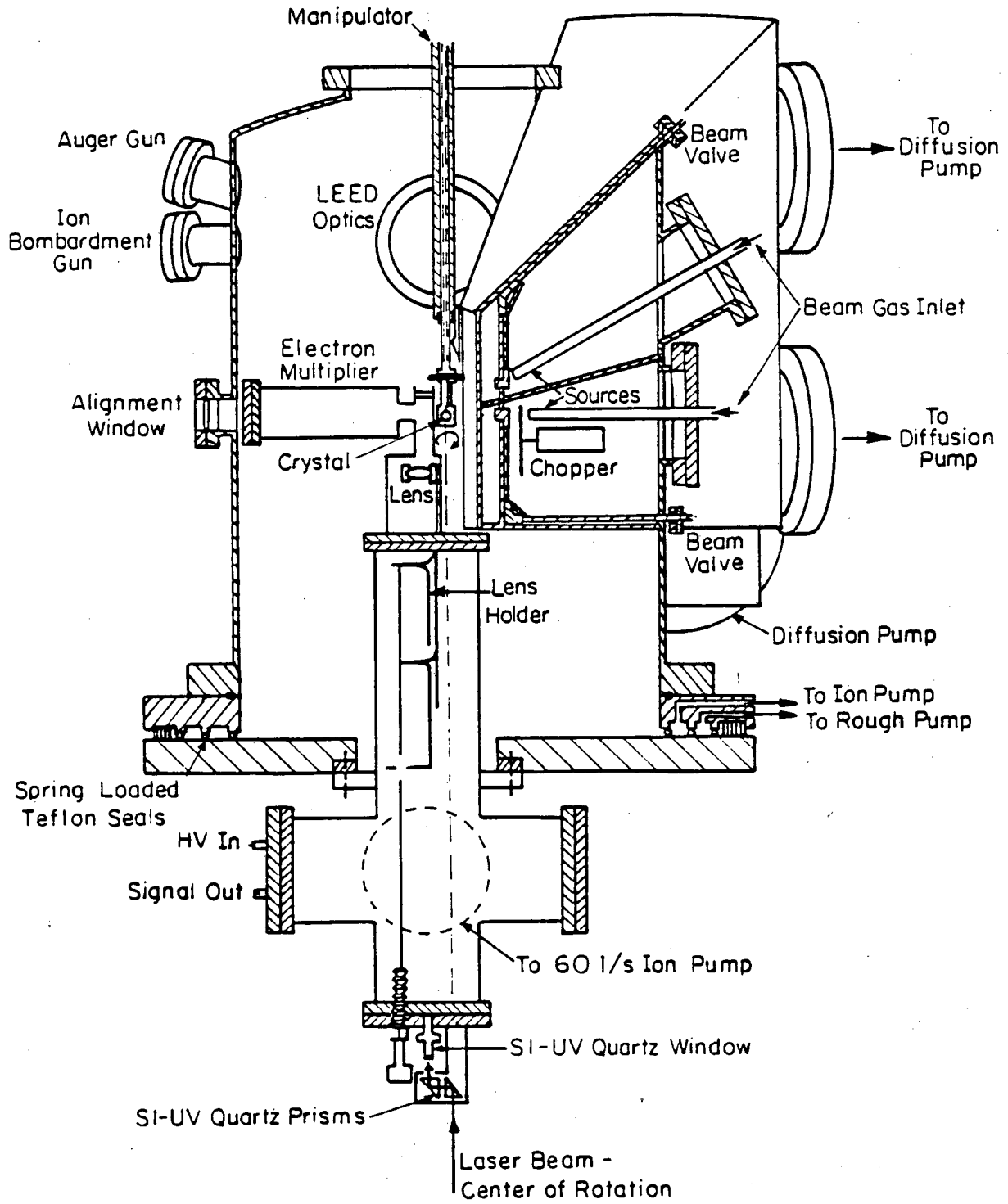
- Fig. 1: Molecular beam-surface scattering laser-induced ionization apparatus.
- Fig. 2: Two photon ionization spectra. The assignment represents a one photon rovibronic absorption of the $A^2\Sigma^+(v' = 0) \leftarrow X^2\Pi_{1/2}(v'' = 0)$ transition. a) Incident supersonic beam of NO molecules. b) Room temperature ambient NO gas at 5×10^{-8} torr. c) Scattered NO molecules from a Pt(111) crystal surface at 580K.
- Fig. 3: Rotational distribution analysis. $N(j'')$ are the rotational line intensities and $E_{\text{rot}} = B''J''(J'' + 1)$ is the rotational energy. The slope determines a rotational temperature. The filled circles are the data measured with the detector at the normal to the crystal surface. The open circles are the data measured with the detector at specular angle -62° from the normal to the surface. In both experiments the crystal temperature is 580K.
- Fig. 4: Rotational temperature of the scattered NO molecules as a function of crystal temperature. The crosses are from spectra taken at the normal to the surface. The circle was taken at specular angle (62° from the normal).
- Fig. 5: Angular distribution of NO molecules in their ground vibrational state after the scattering of a NO seeded He beam (He/NO = 4:1) from the Pt(111) surface. Open circles are NO molecules in rotational states $j'' = 1/2 - 6 1/2$, whereas the filled circles are of NO molecules in the $j'' = 15 1/2$ state. The crystal temperature is 580K. The arrow indicates the specular scattering angle.

Fig. 6: Angular distribution of vibrationally excited ($v'' = 1$) NO molecules scattered from the Pt(111) surface. The arrow indicates the specular scattering angle. The crystal temperature is 820K.

Fig. 7: Vibrational distribution of scattered NO molecules as a function of crystal temperature. The distributions are presented as the ratio of the experimentally measured signals: $\text{NO}(v'' = 1)/\text{NO}(v'' = 0)$. The solid line and open circles are the $\text{NO}(v'' = 0)$ experimental signal (left ordinate). The heavy solid line is the calculated Boltzmann ratio as a function of crystal temperature with $E_v = 1876 \text{ cm}^{-1}$ (right ordinate). Crosses are the normalized (see text) experimental ratios and the dashed line represents the expression $0.67 \exp(-E_v/kT_g)$ where $E_v = 1876 \text{ cm}^{-1}$ and T_g is the crystal temperature.

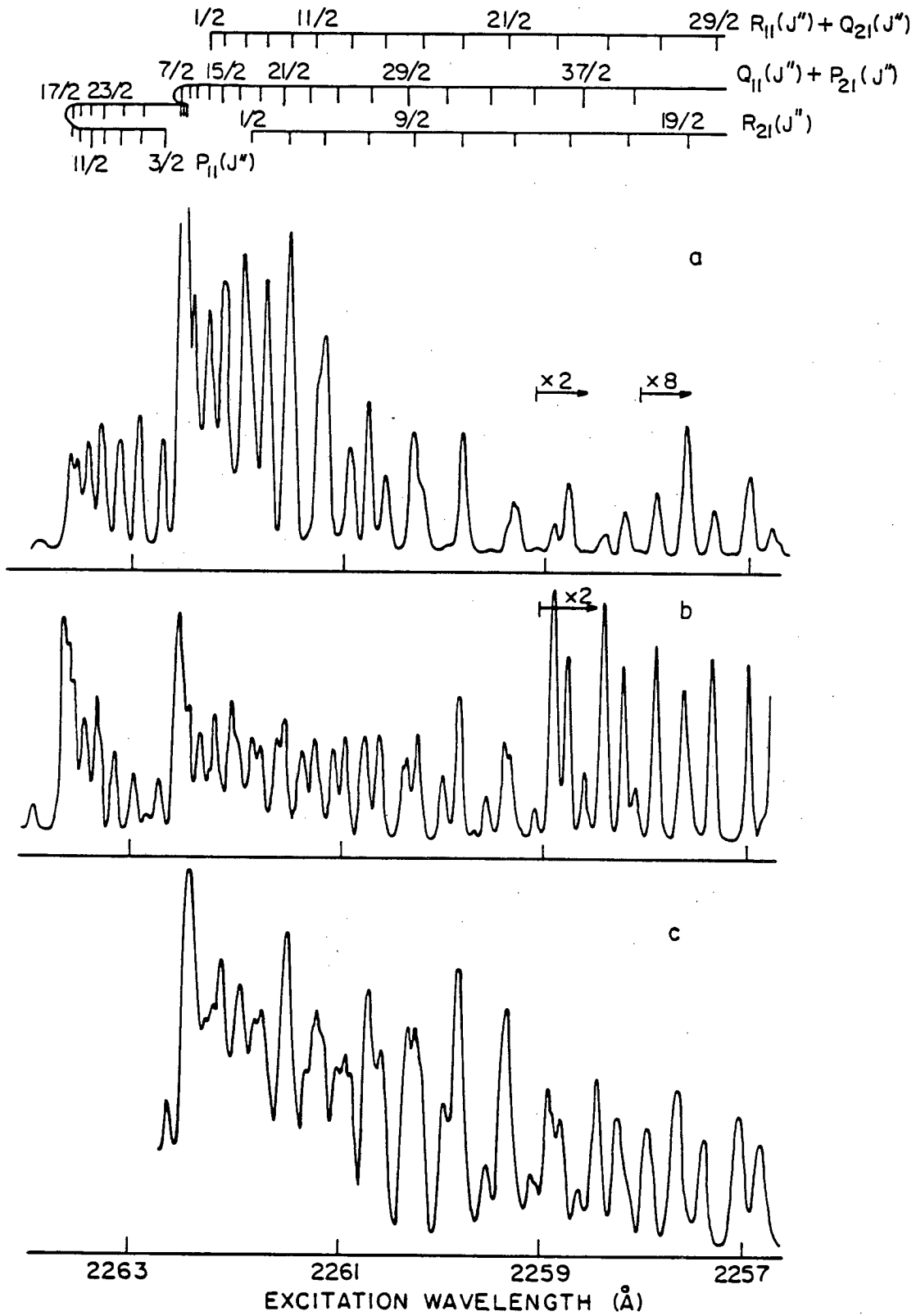
Fig. 8: Vibrational temperature as a function of crystal temperature. The solid line is the expected vibrational temperature if complete accommodation of the desorbed NO molecules with the surface occurs.

Fig. 9: The accommodation coefficient (γ) of the three degrees of freedom of the scattered NO molecules as a function of crystal temperature. The data for translational accommodation is from ref. (2).



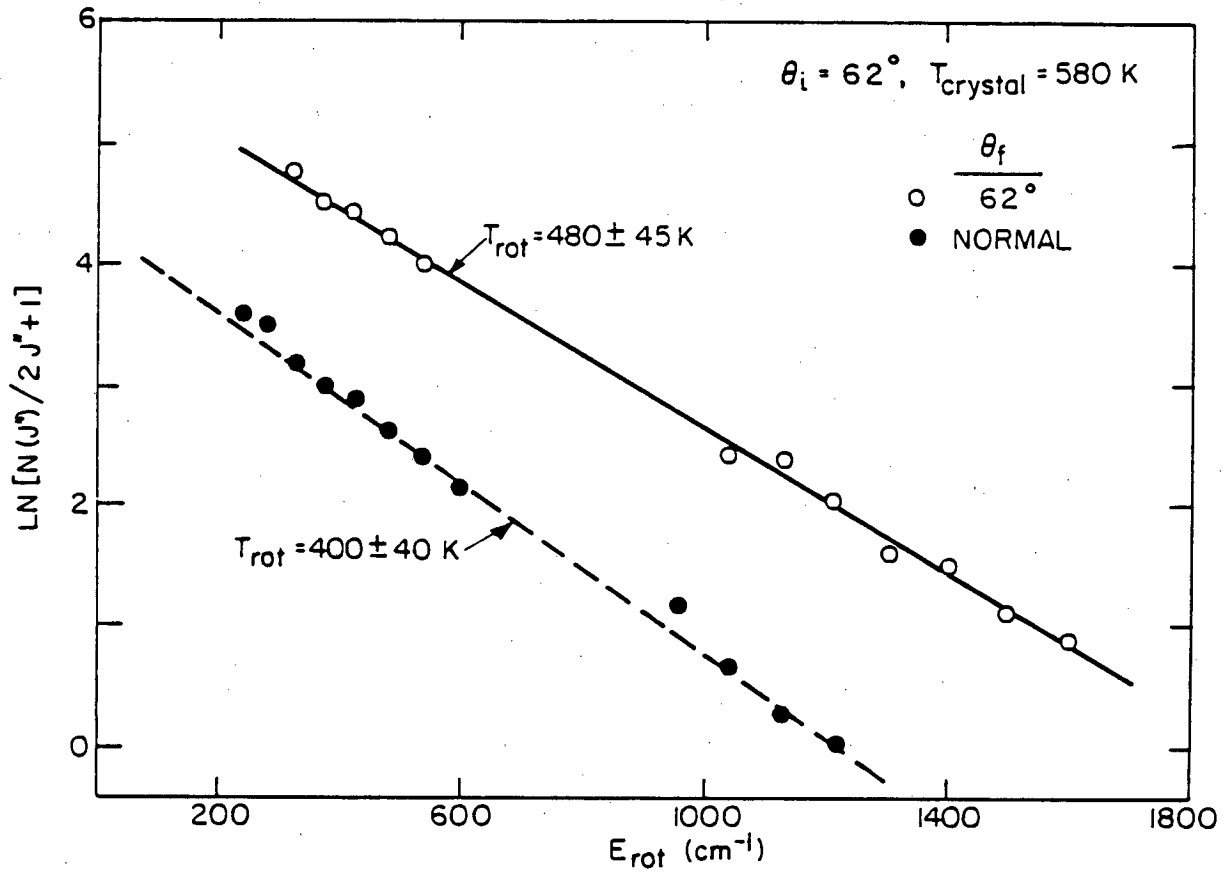
XBL 823-5321

Fig. 1



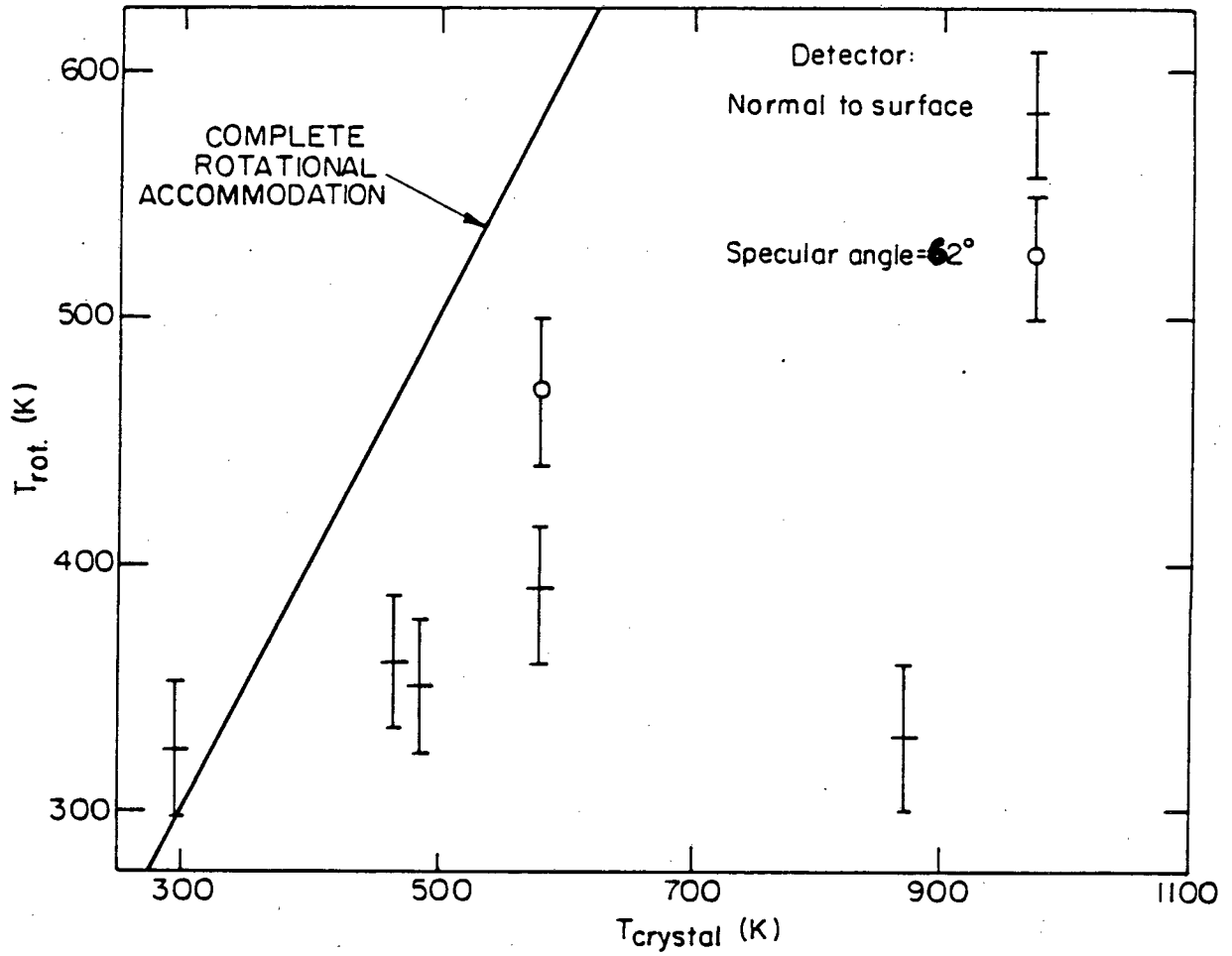
XBL 823-5393

Fig. 2



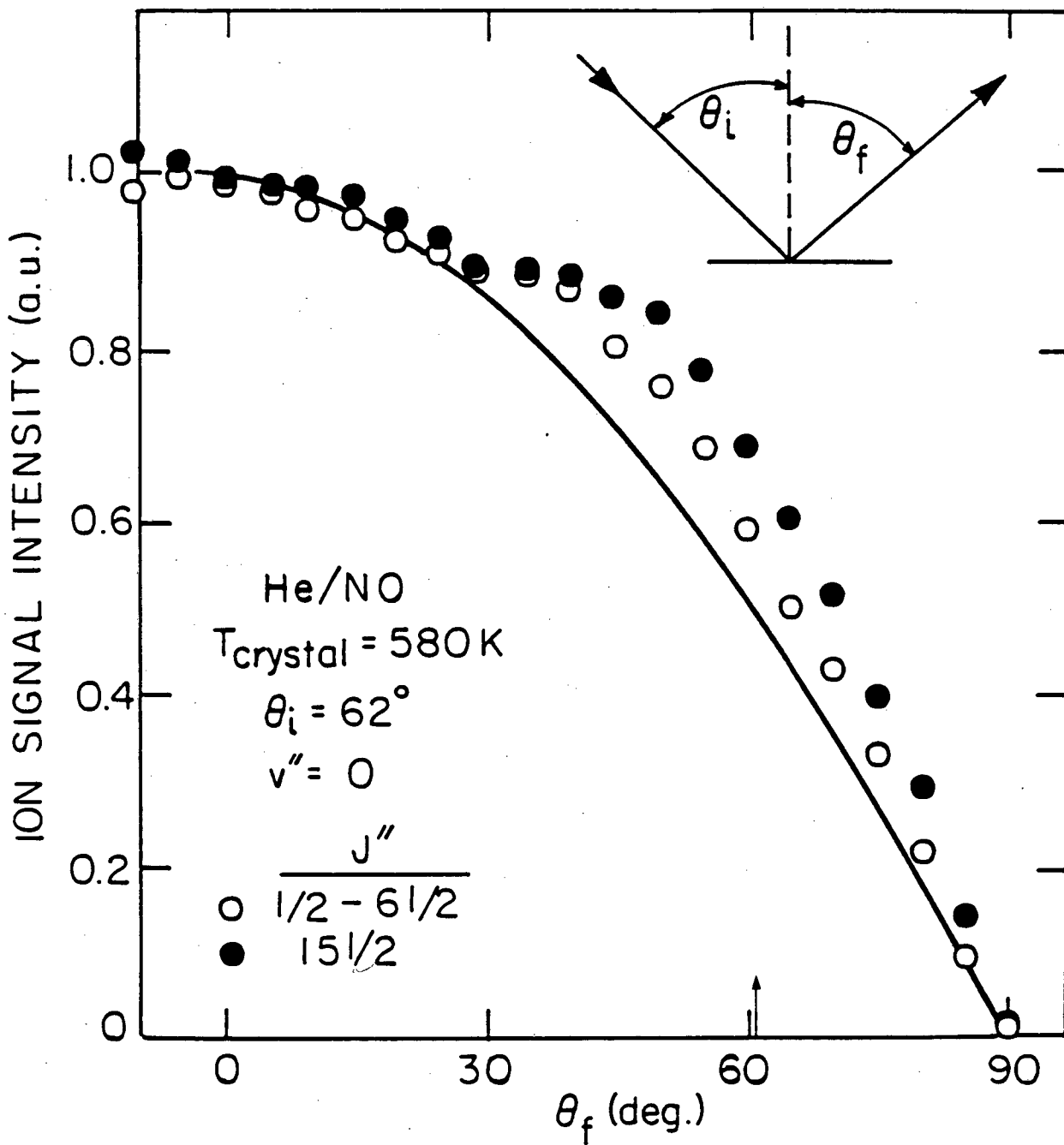
X8L 823-5392

Fig. 3



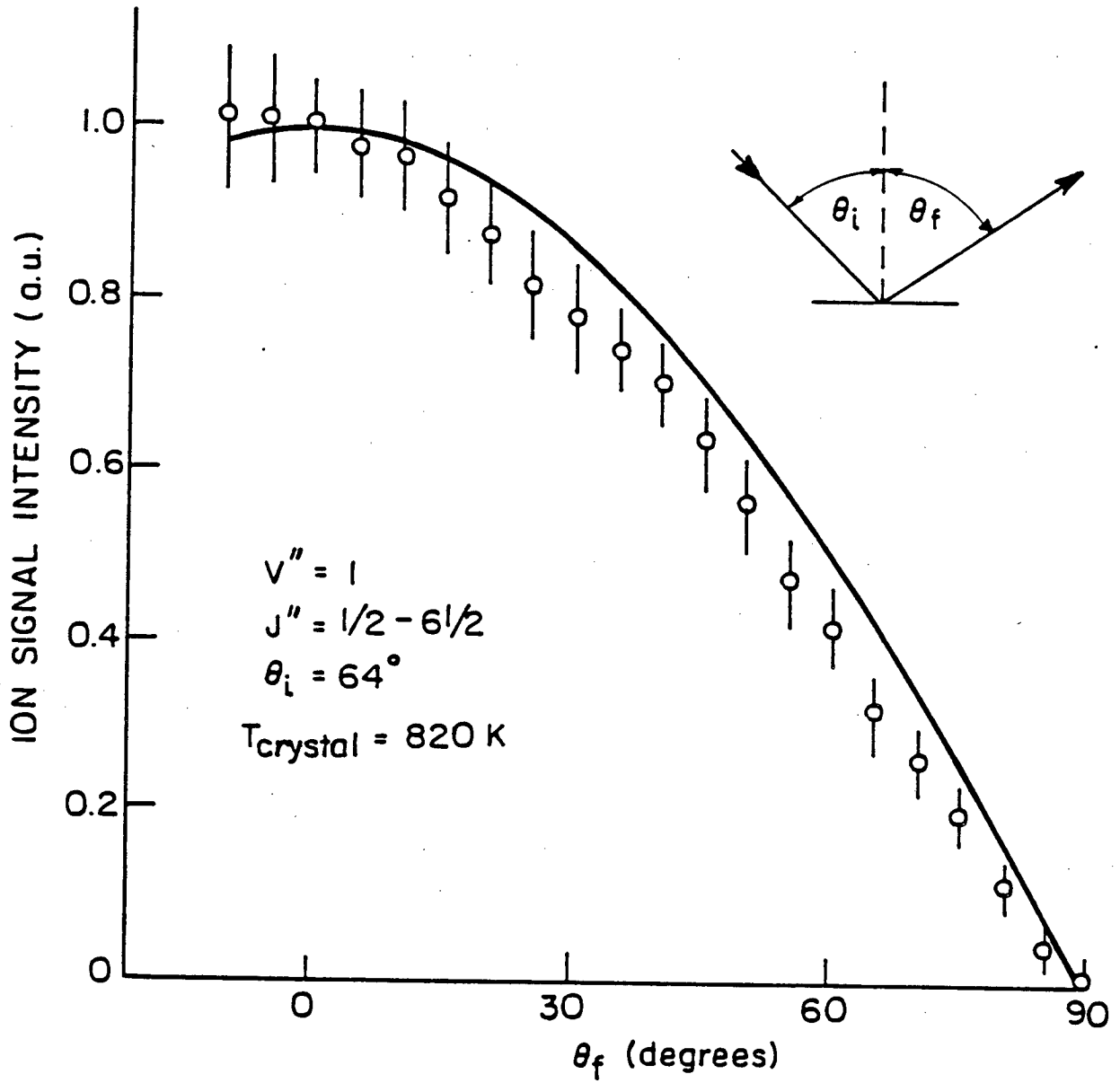
XBL 823-5389

Fig. 4



XBL 827-6042

Fig. 5



XBL823-5322

Fig. 6

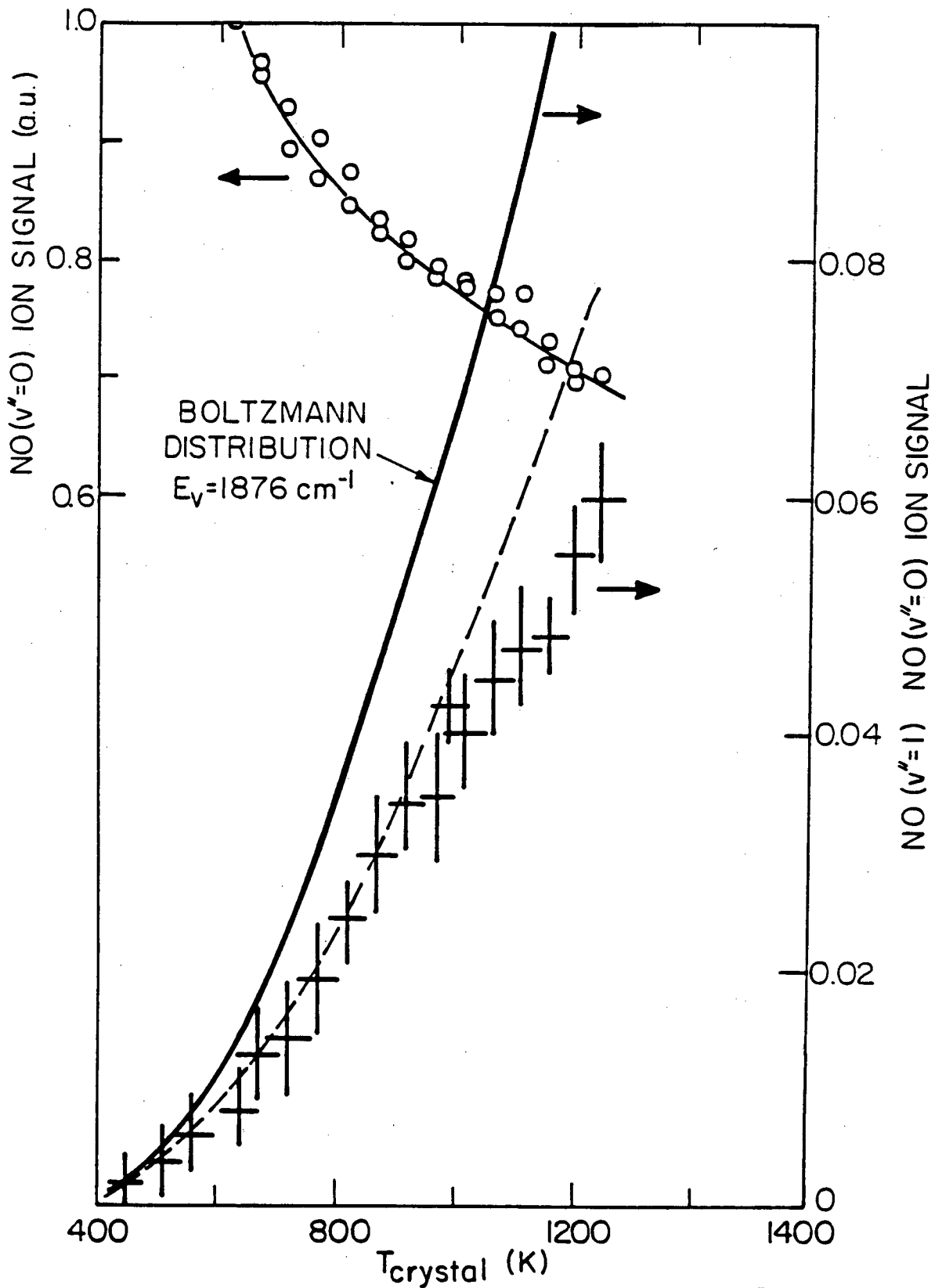
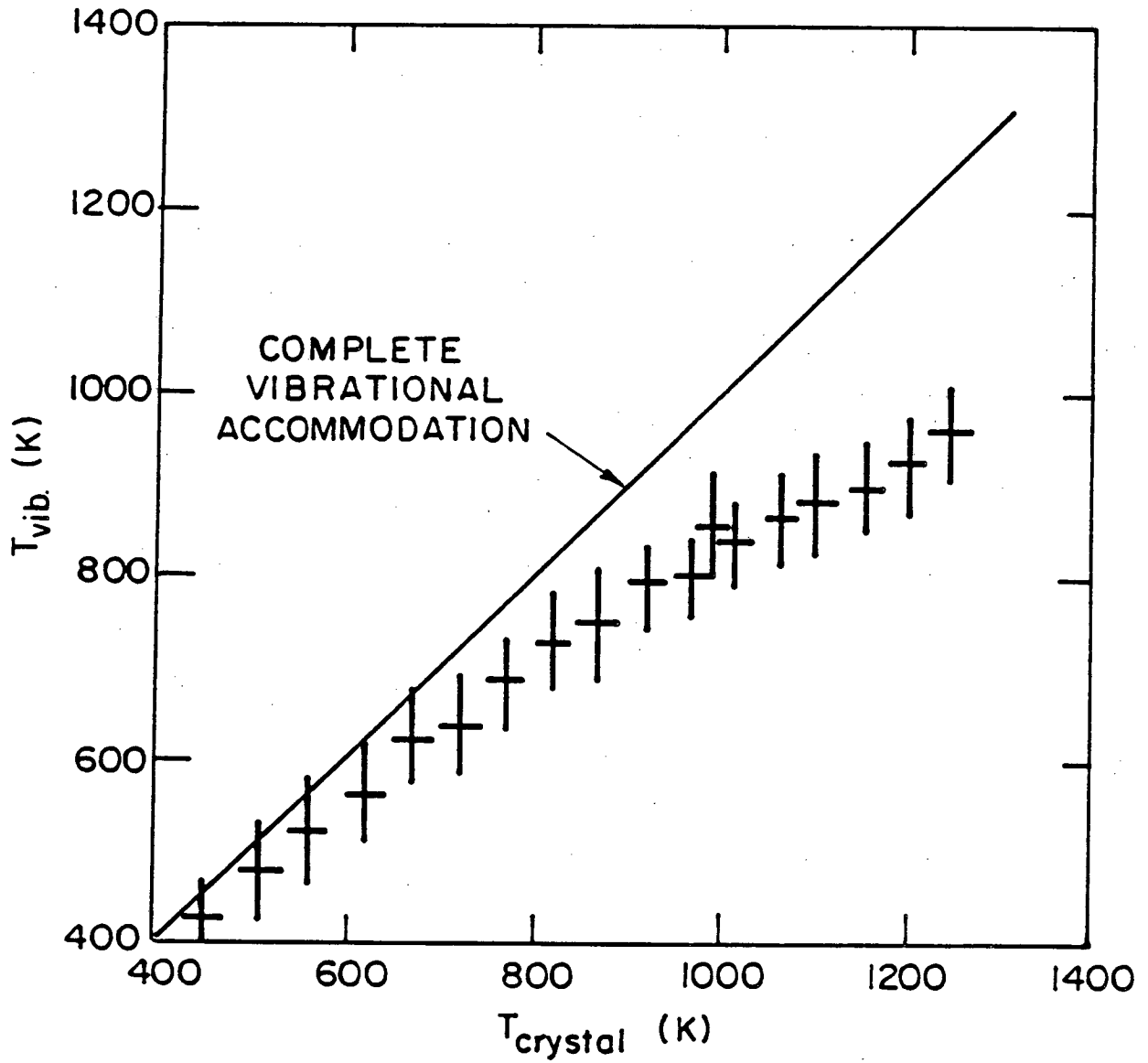


Fig. 7



XBL 827-6041

Fig. 8

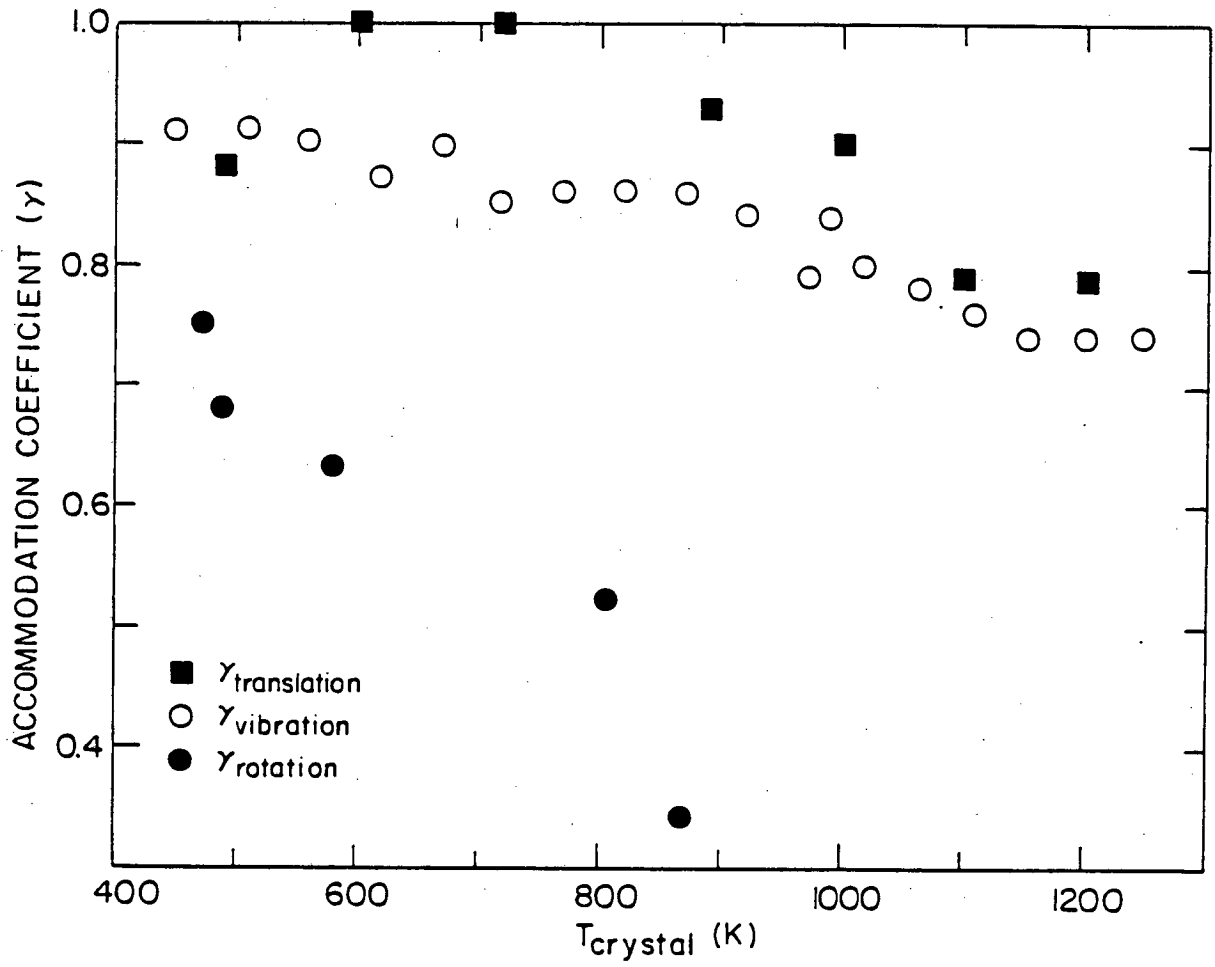


Fig. 9

This report was done with support from the Department of Energy. Any conclusions or opinions expressed in this report represent solely those of the author(s) and not necessarily those of The Regents of the University of California, the Lawrence Berkeley Laboratory or the Department of Energy.

Reference to a company or product name does not imply approval or recommendation of the product by the University of California or the U.S. Department of Energy to the exclusion of others that may be suitable.

TECHNICAL INFORMATION DEPARTMENT
LAWRENCE BERKELEY LABORATORY
UNIVERSITY OF CALIFORNIA
BERKELEY, CALIFORNIA 94720